Journal of Materials Chemistry A

Accepted Manuscript

ROYAL SOCIETY OF CHEMISTRY

www.rsc.org/materialsA

Journal Name

ARTICLE

Received 00th January 20xx,
Accepted 00th January 20xx

DOI: 10.1039/x0xx00000x

www.rsc.org/

Na-Birnessite with High Capacity and Long Cycle Life for Rechargeable Aqueous Sodium-ion Battery Cathode Electrodes

Xueqian Zhang, Zhiguo Hou, Xiaona Li, Jianwen Liang, Yongchun Zhu and Yitai Qian**

Layer structure Na-Birnessite (Na-Bir) $Na_{0.58}MnO_2{\cdot}0.48H_2O$ have been synthesized through a precipitation reaction at room temperature, which is used as rechargeable aqueous sodium-ion battery (RASIB) cathode material for the first time. As RASIB cathode material, the layered Na-Birnessite manifests a high specific capacity of 80 mA h g^{-1} at 1 C without obvious capacity loss after 150 cycles. After heat treatment of Na-Bir sample, it can deliver a specific capacity of 79 mA h g^{-1} at 1 C but only remain 60% of the initial capacity after 150 cycles. The XRD analysis of Na-Bir sample after 150 cycles reveals that the layer structure is remained, while the inductive coupled plasma emission spectrometer-atomic emission spectroscopy (ICP-AES) indicates that dissolution of Mn is merely 0.008 wt.% of Na-Bir after 150 cycles. As cathode electrode in full batteries coupled with $NaTi_2(PO_4)_3$ anode electrode, a high capacity of 39 mA h g^{-1} at 10 C is obtained with capacity retention of 94% after 1000 cycles.

1. Introduction

Rechargeable aqueous sodium-ion battery (RASIB) has received much attention for its using in large scale stationary energy storage systems due to the nontoxic, low cost and nonflammable aqueous electrolyte.[1-3] Only few cathode materials have been explored for RASIB.[2-7] Oxides such as Na_xMnO_2 used as RASIB cathode material could give a capacity of about 50 mA h g^{-1} at 1 C and retain 80% of initial capacity after 1000 cycles.[8-12] Polyanionic compound $Na_2FeP_2O_7$ delivered a higher specific capacity of about 65 mA h g^{-1} at a rate of 1 C with 77% capacity remained after 300 cycles.[13] Song et al. reported that NASICON-type $Na_3V_2(PO_4)_3$ exhibited a capacity of about 50 mA h g^{-1} at 8.5 C and 50% of initial capacity after 30 cycles.[14] Prussian blue analogues $Na_2NiFe^{II}(CN)_6$ showed a discharge capacity of about 60 mA h g^{-1} at a rate of 1 C.[15, 16, 17]

Among these RASIB cathode materials, Mn-containing materials have been of particular interest because of the low cost and abundance of raw materials.[10-12, 18, 19] A full cell using tunnel-type $Na_{0.44}MnO_2$ as cathode material and $NaTi_2(PO_4)_3$ as anode material could deliver a specific capacity of approximately 25 mA h g^{-1} (based on total mass of cathode and anode active materials) with 50% retention after 1600 cycles at 7 C.[12] When coupled with $NaTi_2(PO_4)_3$ to assemble a full battery, $NaMnO_2$ gave a discharge capacity of 37 mA h g^{-1} at a rate of 1 C and remained 75% of initial capacity after 500 cycles.[18] Chen's group has reported a full cell using $Na_{0.66}Mn_{0.66}Ti_{0.34}O_2$ as cathode and $NaTi_2(PO_4)_3$ as anode, which the battery exhibited a reversible capacity of 46 mA h g^{-1} at a rate of 2 C with capacity retention of 89% after 300 cycles. However, the serious problem Mn-containing materials encountered is the structural instability during repeated charge/discharge cycles, which results in the fast capacity fading.[18, 20]

Layer-type Birnessite with crystal water has been demonstrated as an effective approach to overcome this shortcoming in nonaqueous electrolyte sodium-ion batteries duo to its stable layer structure.[21, 22] Layer structure Birnessite with crystal water $Na_{0.71}MnO_2 \cdot 0.25H_2O$ could remain 94.4% of initial capacity after 30 cycles at 1/15 C superior than that without crystal water after heat treatment, which retained only 51% of the initial capacity.[21]

In this work, we synthesized layer Na-Birnessite $Na_{0.58}MnO_2{\cdot}0.48H_2O$ (Na-Bir) used as RASIB cathode material through a precipitation reaction at room temperature. In aqueous electrolyte, the as-prepared electrodes give a high reversible capacity of about 80 mA h g^{-1} at 1 C rate with 100% of initial capacity

Hefei National Laboratory for Physical Science at Microscale, Department of Chemistry, University of Science and Technology of China
96 JinZhai Road, 230026, Hefei, China
E-mail: ytqian@ustc.edu.cn, ychzhu@ustc.edu.cn.

†Electronic Supplementary Information (ESI) available: XRD pattern of the Na-Bir after heat treated; XPS analysis of Na-Bir, Cyclic voltammetry results of sample; Warburg constant plots of Na-Bir and heat treated Na-Bir materials; Thermogravimetric analysis of Na-Bir and PVDF; Capacity and cycle performance of RASIB cathode materials. See DOI: 10.1039/x0xx00000x

retention after 100 cycles in a voltage range of -0.1 - 0.8 V vs. Ag/AgCl. After 1000 cycles at a current density of 10 C, it delivers a high capacity of 62.5 mA h g^{-1} with 100% of initial capacity remained. Even at a very high rate of 50 C, the electrode still exhibits a high discharge capacity of 54 mA h g^{-1}. For comparison, the Na-Bir without crystal water treated by annealing remains only 60% of initial discharge capacity after 150 cycles at a rate of 1 C. XRD analysis at different voltage and after 150 cycles was conducted. It is found that the layer with crystal water structure was well maintained. The inductive coupled plasma emission spectrometer-atomic emission spectroscopy (ICP-AES) results demonstrate that there is merely 0.008 wt.% of Mn dissolution in aqueous electrolyte. What's more, after coupled with $NaTi_2(PO_4)_3$, the full cell exhibits a high reversible capacity of 50 mA h g^{-1} at a current density of 1 C with capacity retention of 94% after 1000 cycles at 10 C. The good electrochemical performance suggests that the layer Na-Bir should be a promising cathode material for RASIB.

2. Materials and methods

2.1. Materials synthesis

Na-Birnessite (Na-Bir) was synthesized by a facile precipitation reaction. All of the chemicals purchased from Sino-reagent were analytically pure and used without further purification. 5.377 g $MnSO_4$ (50 wt%) solution was dissolved in 50 mL distilled water to form a light pink solution (solution A). 2.16 g NaOH was dissolved in 90 mL distilled water with 10 mL H_2O_2 (30 wt%) solution added to form a clear solution (solution B). Then the solution B was added into solution A drop by drop with vigorous magnetic stirring for 2 h. Next the brown suspension was aged at room temperature overnight. After that, the supernatant was poured out and the deposit was filtered and washed by distilled water and ethanol three times. The black powder was dried at 50 ^oC overnight then the Na-Bir material was obtained. The annealing Na-Birnessite (heat treated Na-Bir) was prepared by heating Na-Bir at 300 ^oC in N_2 for 5 h.

2.2. Characterization

The X-ray powder diffraction (XRD) patterns of the as-prepared materials were conducted on a Philips X'pert X-ray diffractometer with Cu Ka radiation (λ = 1.54182 Å) at a scan rate of 0.08842^o s^{-1} with a ramping step of 0.02^o. The morphology of products was characterized by field-emitting scanning electron microscope (FESEM, JEOL-JSM-6700F) and transmission electron microsocopy (TEM, Hitachi H7650 and HRTEM, JEOL 2010). The molar ratio of Na and Mn element was measured by inductive coupled plasma emission spectrometer-atomic emission spectroscopy (ICP-AES, Optima 7300DV). The thermogravimetric analysis (TG) carried out from room temperature to 300 ^oC at a heating rate of 10 ^oC min^{-1} under N_2 flow. X-ray photoelectron spectroscopy (XPS) analysis was carried out on a Thermo Scientific Kα spectrometer (monochromatic Al Kα, 1486.6 eV).

2.3. Electrochemical measurements

The electrochemical performances of the Na-Bir were tested using three-electrode cells. One larger piece of pure titanium sheet and an Ag/AgCl electrode (0.197 V vs. NHE) were used as counter and reference electrode, respectively. The working electrode active material, super P carbon black and polyvinylidene fluoride (PVDF) binder (5 wt%) were hand ground in a weight ratio of 70 : 20 : 10. The slurry was cast onto titanium mesh (100 mesh) with about 1 cm^{-2} area. The as-prepared electrodes were then dried at 110 ^oC for 10 h in a vacuum oven. The typical loading of the active material was about 10 mg cm^{-2}. The electrolyte was 1mol L^{-1} Na_2SO_4 aqueous solution without purged with N_2. Galvanostatic charging–discharging tests were conducted on a LAND cycler (Wuhan Kingnuo Electronic Co., China) at room temperature with 1 C corresponding to 80 mA g^{-1}. Cyclic voltammetry (CV) curves were performed on a CHI 660E electrochemical workstation (Shanghai).

3. Results and discussion

Fig. 1a shows the XRD pattern of as-synthesized Na-Bir, which can be indexed to layer hexagonal unit cell with Birnessite framework of P63/mmc space group.[22] The manganese oxide (MO) layer-to-layer distance is approximately 7.12 Å based on the (002) diffraction peak, which is in good agreement with previous report.[21] The (004) diffraction peak located at about 25.3^o suggests the interplanar spacing is about 3.52 Å which should be ascribed to manganese oxide layer to water (or Na ion).[22, 23] The peak located at about 37^o might indicate a turbostratic structure of Na-Bir, which should ascribe to the disordered atomic distributions in the lattice planes with h or k ≠ 0.[21,23] XRD pattern of the

Na-Bir after heat treated (Fig. S1†) shows that the (002) peak is located at 15.6° indicating the interplanar distance is 5.66 Å, the MO layer spacing distance decreases dramatically from 7.12 Å to 5.66 Å for Na-Bir and Na-Bir after heat treated, which indicates the structural influence of crystal water.[21] What's more, the (004) diffraction peak is weakened and hardly to be seen. The morphology of Na-Bir was characterized by field-emitting scanning electron microscope (FE-SEM). As shown in Fig. 1b, the Na-Bir is composed of wrinkled thin sheets. More structure details were obtained from transmission electron microsocopy (TEM) image, in which the thickness of wrinkled sheets is about 10 nm (as shown in Fig. 1c).

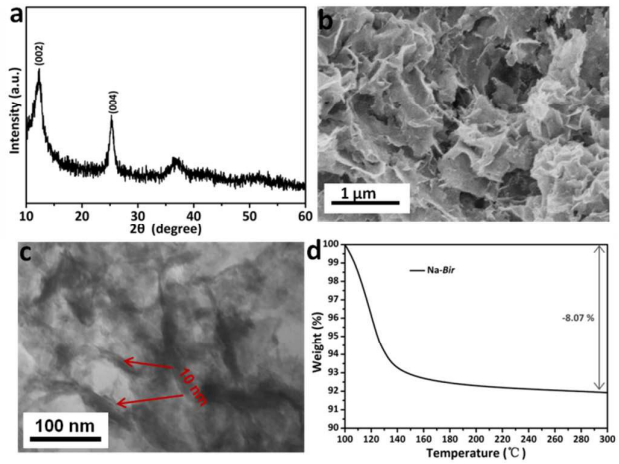

Fig. 1 (a) XRD pattern of the as-prepared Na-Bir sample, (b) and (c) SEM and TEM images of the Na-Bir, (d) TG profile of Na-Bir from 120 to 300 °C.

The exact amount of crystal water in the Na-Bir was inferred by conducted thermogravimetric analysis (TG) from room temperature to 300 °C at a ramping rate of 10 °C min^{-1} under N_2 flow. The weight loss happened mainly at 120 °C, which is ascribed to the typical departure of crystal water.[22] The overall weight loss of the Na-Bir is about 8.07%, ascribed to the crystal water evaporation during heat treatment.[24] The ratio of Na and Mn element was tested by using ICP-AES. According to the ICP-AES results, the ratio of Na and Mn element is 0.58. From the above, the chemical formula of the as-synthesized Na-Bir is $Na_{0.58}MnO_2 \cdot 0.48H_2O$, which indicates that the valence of the Mn is approximately +3.42. To further investigate the oxidation state of Mn, the X-ray photoelectron spectroscopy (XPS) analysis was carried out (Fig. S2†). The measurement reveals the ratio of Mn^{3+} and Mn^{4+} is about 10:7 and the average valence of Mn is about 3.4, which is close to the result of ICP-AES analysis.

Electrochemical characterization was carried out using three electrode cells. The charge and discharge profiles of Na-Bir electrode during the first five cycles were measured at a current density of 1 C rate (as shown in Fig. 2a), which exhibits a flat discharge platform at about 0.45 V. Two well-defined charge plateaus are located at about 0.6 and 0.75 V and a tiny platform emerges at 0.05 V. The first charge capacity is about 68 mA h g^{-1} and the subsequent four cycles give a reversible capacity of 80 mA h g^{-1} with high coulombic efficiency of 100%. The voltage profiles are indeed consistent with the cyclic voltammetry (CV) data. As shown in Fig. S3a†, there are three oxidation peaks during cathodic scan. One tiny peak is located at 0.05 V and a broad peak is observed at 0.75 V with a shoulder near 0.6 V. During anodic scan, one broad reduction peak is observed at 0.45 V. However, the sample of Na-Bir after heat-treatment performs totally different electrochemical characteristics. The CV profiles exhibit ideal rectangular shape, which indicate the electric double layer capacitance characteristic of heat treated Na-Bir (Fig. S3b†). With the crystal water extracted, the MO layer space is shrunk which impedes the Na ion (de)intercalated from/into the interlayer space.[22]

The Na-Bir containing crystal water exhibits high rate capability in aqueous electrolyte as shown in Fig. 2b. The electrode gives a high specific capacity of 80 mA h g^{-1} at 1 C rate. The capacity retains 73, 67, 61 and 57 mA h g^{-1} when the current density is increased to 2, 5, 10 and 20 C, respectively. It's remarkable that, even as the current density is increased to a very high rate of 50 C, the electrode still deliver a reversible capacity of 54 mA h g^{-1}. Besides good rate capability, the Na-Bir shows long cycle life during repeated charge-discharge cycles. When tested at a high rate of 10 C, its initial discharge capacity is 62.4 mA h g^{-1} and remain 62.5 mA h g^{-1} capacity with almost no capacity loss after prolonged 1000 cycles. Combined with the high specific capacity, the Na-Bir can be comparable to those cathode materials which exhibit the best performance.[17] The cycle performance of Na-Bir after heat-treatment was also examined. It delivers 79 mA h g^{-1} initial discharge capacity at 1 C rate. However, the capacity retention is only 60% after 150 cycles. The Na-Bir gives an 80 mA h g^{-1} initial discharge capacity without capacity decay after 150 cycles.

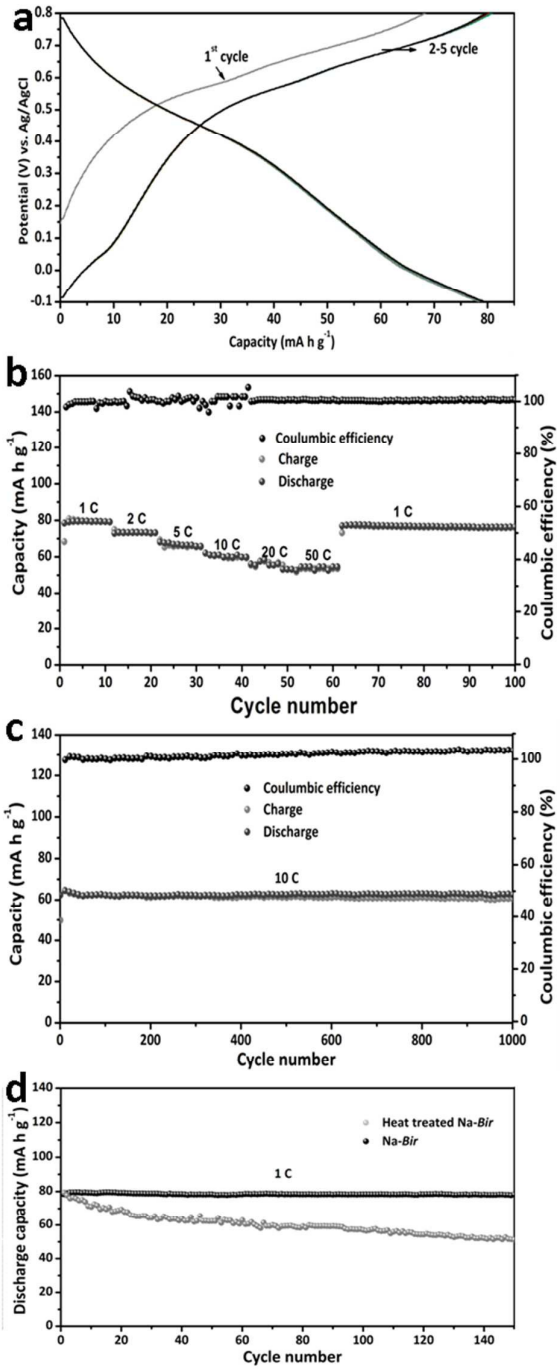

Fig. 2 (a) Charge/discharge profiles of Na-Bir at a rate of 1 C, (b) rate capability of the Na-Bir from 1 C to 50 C, (c) long cycle performance of Na-Bir electrode at a rate of 10 C. (d) Cycle performance at 1 C of Na-Bir and heat treated Na-Bir electrodes, respectively.

The electrochemical performance suggest that the Na-Bir shows superior Na ion storage properties than that of heat treated Na-Bir. Further analysis involved electrochemical impedance spectroscopic (EIS) analysis, XRD patterns and ICP-AES measurements were collected to understand the structure changes during cycles deeper.

EIS measurement was conducted to compare Na-Bir with Na-Bir after heat-treatment in Na storage characteristics. As shown in Fig. 3a, the diameter of the semicircle for Na-Bir in the high frequency region designated to the charge transfer resistance (R_{ct}) between the electrolyte and the active material is only half of that for heat treated Na-Bir. That is to say, the layered Na-Bir possesses much smaller charge transfer resistance than heat treated Na-Bir. Na ion diffusion kinetics difference of Na-Bir and heat treated Na-Bir was certified by Warburg constant σ. Warburg constant σ is the slope of Z ' with $\omega^{-1/2}$ ($\omega = 2\pi f$) at low frequency.[25] The plotting of σ (shown in Fig. S4†) reveals that the Na ion diffusion resistance of heat treated Na-Bir is almost three times higher than that of Na-Bir, which indicates that Na ion could be diffused easily among NB structure. The EIS results clearly show that crystal water not only decreases the charge transfer resistance, but also improves the Na ion conductance during charge/discharge cycles. Due to the crystal water, the interlayer space is increased which facilitates Na ion diffusion in the Na-Bir structure.[21]

XRD patterns of Na-Bir and heat treated Na-Bir electrodes were carried out to find out whether the structure changes or not after charge/discharge cycles. It is obvious to see that all the characteristic peaks are preserved (Fig. 3b), which unambiguously confirms that the crystal structure of Na-Bir is well remained. The clearly visible (004) peak demonstrates that the crystal water positions in between the MO layers. However, the characteristic diffraction peaks of heat treated Na-Bir vanish after 150 cycles, indicating that its structure was collapsed. The XRD results confirm that the layer structure of Na-Bir is much more stable than heat treated Na-Bir during charge/discharge cycles.

Inspired by the stable structure of Na-Bir after long cycles, deep works are performed to further understand the Na-Bir structure changes during Na ion insertion/extraction. The ex situ XRD analysis was collected during the charge/discharge cycle under a current rate of 0.5 C at a voltage range between -0.1 and 0.8 V (Fig. 3c). The (002) reflection reveals continuous peak shift during Na extraction. After fully

charged to 0.8 V, the 002 peak slightly shift from 12.43° to 12.04°, while the interlayer space between MO layers only stretches a little (3.17%). Notable angle shifts are observed in the X-ray diffraction patterns at a voltage range from 0.45 to 0.8 V corresponding to the lattice parameter expands continuously, which should ascribe to the Na ion extraction that results in the MO interlayer repulsion of each other.[21, 23] Even though a lot of Na ions are extracted, the Na-Bir can be stabilized in layer structure. The whiff lattice expansion of the Na-Bir suggests that there is small tension during Na ion extracted from layer framework, which the crystal water acts as a cushion. When discharged at 0.5 C, the peak of (002) shifts from 12.04° to 12.45°. During the charge/discharge process, the peak transition exhibits a symmetric behaviour. It is demonstrated that the layer structure with crystal water is very stable during Na ion extraction and insertion process, which should be the main reason of the long cycle stability. The TG analysis of the Na-Bir after 150 cycles verifies the existence of the crystal water and remains almost the same content as pristine sample (as shown in Fig. S5a† and S5b†). In contrast, the heat treated Na-Bir exhibits almost no signal of crystallinity without any visible diffraction peaks. These results strongly demonstrate the crystal water play a crucial role on the structure stability. If not crystal water, the structure integrity will be decomposed and the layer framework will be damaged.

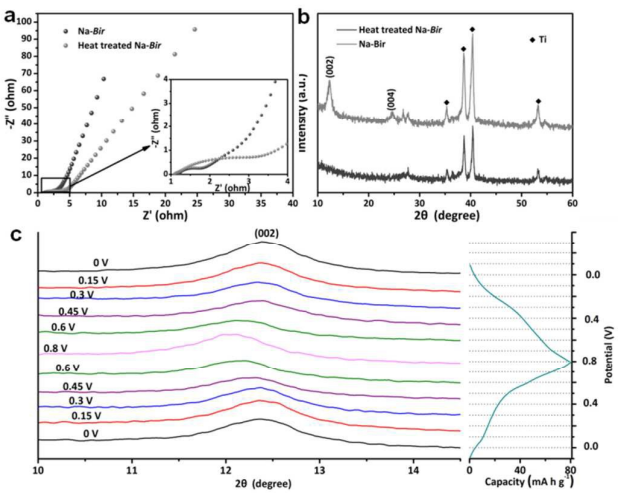

Fig. 3 (a) Nyquist plots for Na-Bir and heat treated Na-Bir materials, (b) XRD patterns of Na-Bir and heat treated Na-Bir after 150 cycles at a rate of 1 C, (c) Ex situ XRD patterns collected during charge process under a current density of 0.5 C at a voltage range between -0.1 to 0.8 V.

Mn dissolution is also a serious problem of the Mn-containing materials.[8, 21, 26] ICP-AES measurement was conducted to detect the Mn dissolution behavior of Na-Bir in aqueous electrolyte. According to the analysis results, after 150 cycles of Na-Bir electrode, the concentration of Mn in electrolyte is about 0.007 μg mL^{-1}. The Mn dissolved in water corresponds to 0.008 wt.% of the active material. However, the dissolution of Mn of heat treated Na-Bir in aqueous electrolyte is very serious. The concentration is about 2000 times higher than Na-Bir. The crystal water releases the structure strain during Na ion intercalation/extraction into/from the later framework, which dramatically suppresses the dissolution of Mn.[21, 23, 24]

EIS results reveal that Na-Bir electrodes possess much smaller charge transfer resistance and higher Na ion diffusion conductivity, which result in higher rate capability than that of heat treated Na-Bir. XRD results show that the structure Na-Bir is very stable during long cycling performance. ICP-AES measurement exhibits that there is almost no Mn dissolution, which suggests that Na-Bir is stable in the aqueous electrolyte. The robust structure and suppressed dissolution of active material in electrolyte are main reasons of the long cycle life.[3,4,27]

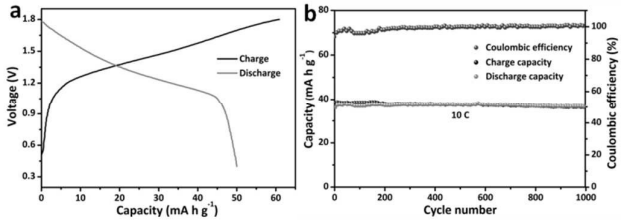

Fig. 4 (a) The typical charge/discharge profiles of Na-Bir/ $NaTi_2(PO_4)_3$ full cell at 1 C in the voltage range of 0.4 and 1.8 V, (b) Cycling performance of Na-Bir/ $NaTi_2(PO_4)_3$ full cell at a high rate of 10 C.

Thereafter, a full cell was assembled using $NaTi_2(PO_4)_3$ as anode material [18] and Na-Bir as cathode material, and its electrochemical performance was evaluated. The active material loading of anode electrodes was about 5.8 mg cm^{-2} and the weight ratio of cathode and anode active material was about 1.7. The capacity of the full battery is based on the total mass of cathode and anode active materials. 1 M Na_2SO_4 aqueous electrolyte was purged with N_2 flow for 2 h before use to remove the dissolved O_2. Before assembling, the cathode material was charged and

discharged for one cycle to activate the electrode. The typical charge-discharge files of the full cell are shown in Fig. 4a. The full cell cycled at a voltage window between 0.4 and 1.8 V exhibits a high discharge capacity of about 50 mA h g^{-1} at a current density of 1 C. The cell gives an average operating voltage of 1.4 V, which is higher than that of $Na_{0.44}MO_2$. The Na-Bir/$NaTi_2(PO_4)_3$ full battery shows a high stable cycling performance over 1000 cycles as shown in Fig. 4b. It delivers a reversible capacity of 39 mA h g^{-1} at a high rate of 10 C and with only 5.8% capacity loss after 1000 cycles. The cycle performance and rate capability of the Na-Bir are very remarkable among the RASIB cathode materials which have been reported (listed in Table S1).[12, 16,17, 19, 28]

4. Conclusions

In summary, we have prepared layer $Na_{0.58}MnO_2{\cdot}0.48H_2O$ with high specific capacity and good rate capability by a simple precipitation process. From the XRD analysis, it is concluded that Na-Bir retains structure integrity after long cycles. Very few dissolution of Mn was demonstrated by ICP-AES measurement, which suggests high stability of Na-Bir in aqueous electrolyte. Compared with Na-Bir after heat treatment, the Na-Bir possess much better sodium storage performance, which should be resulted from its unique stable layered structure. Our work is expected to open a new avenue that Na-Bir and its analogue which contain stable crystal water can be used as RASIB cathode materials for large scale grid energy storage systems.

Acknowlagements

This work was financially supported by the Foundation for Innovative Research Groups of the National Natural Science Foundation of China (Grant 21521001), the National Natural Science Fund of China (No. 21471142, 2120115 8) and the authors thank the Specialized Research Fund for the Doctoral Program of Higher Education of China.

Notes and references

[1] M. Armand, J. M. Tarascon, *Nature,* 2008, **451**, 652.
[2] H. Kim, J. Hong, K. Y. Park, H. Kim, S. W. Kim, K. Kang, *Chem. Rev.,* 2014, **114**, 11788.
[3] W. Li, J. Dahn, D. Wainwright, *Science,* 1994, **264**, 1115.
[4] J.-Y. Luo, W.-J. Cui, P. He, Y.-Y. Xia, *Nat. chem.,* 2010, **2**, 760.
[5] a) H. Manjunatha, G. Suresh, T. Venkatesha, *J. Solid State*. *Electrochem.,* 2011, **15**, 431; b) W. Li, W. McKinnon, J. Dahn, *J. Electrochem. Soc.*,1994, **141**, 2310.
[6] Y. Fang, L. Xiao, X. Ai, Y. Cao and H. Yang, *Adv. Mater.*, 2015, **27**, 5895.
[7] Y. Cao, L. Xiao, W. Wang, D. Choi, Z. Nie, J. Yu, L. V. Saraf, Z. Yang and J. Liu, *Adv. Mater.*, 2011, **23**, 3155.
[8] L. Athouël, F. Moser, R. Dugas, O. Crosnier, D. Bélanger, T. Brousse, *J. Phys. Chem. C,* 2008, **112**, 7270.
[9] Q. Qu, Y. Shi, S. Tian, Y. Chen, Y. Wu, R. Holze, *J. Power Sources,* 2009, **194**, 1222.
[10] J. Whitacre, A. Tevar, S. Sharma, *Electrochem. Commun.,* 2010, **12**, 463.
[11] J. Whitacre, T. Wiley, S. Shanbhag, Y. Wenzhuo, A. Mohamed, S. Chun, E. Weber, D. Blackwood, E. Lynch-Bell, J. Gulakowski, *J. Power Sources*, 2012, **213**, 255.
[12] Z. Li, D. Young, K. Xiang, W. C. Carter, Y. M. Chiang, *Adv. Energy. Mater.,* 2013, **3**, 290.
[13] Y. H. Jung, C. H. Lim, J. H. Kim, D. K. Kim, *RSC adv.,* 2014, **4**, 9799.
[14] W. Song, X. Ji, Y. Zhu, H. Zhu, F. Li, J. Chen, F. Lu, Y. Yao, C. Banks, *ChemElectroChem,* 2014, **1**, 871.
[15] a) X. Wu, Y. Luo, M. Sun, J. Qian, Y. Cao, X. Ai, H. Yang, *Nano Energy,* 2015, **13**, 117; b) C. D. Wessells, S. V. Peddada, M. T. McDowell, R. A. Huggins, Y. Cui, *J. Electrochem. Soc.,* 2011, **159**, A98.
[16] a) X. Wu, Y. Cao, X. Ai, J. Qian, H. Yang, *Electrochem. Commun.,* 2013, **31**, 145; b) X. y. Wu, M. Sun, Y. Shen, J. Qian, Y. Cao, X. Ai, H. Yang, *ChemSusChem,* 2014, **7**, 407.
[17] a) C. D. Wessells, S. V. Peddada, R. A. Huggins, Y. Cui, *Nano lett.,* 2011, **11**, 5421; b) C. D. Wessells, R. A. Huggins, Y. Cui, *Nat. commun.,* 2011, **2**, 550; c) M. Pasta, C. D. Wessells, N. Liu, J. Nelson, M. T. McDowell, R. A. Huggins, M. F. Toney, Y. Cui, *Nat. commun.,* 2014, **5**, 3007.
[18] Z. Hou, X. Li, J. Liang, Y. Zhu, Y. Qian, *J. Mater. Chem. A,* 2015, **3**, 1400.
[19] Y. Wang, L. Mu, J. Liu, Z. Yang, X. Yu, L. Gu, Y. Hu, H. Li, X. Yang, L. Chen, X. Huang, *Adv. Energy. Mater.,* 2015.
[20] S. Komaba, A. Ogata, T. Tsuchikawa, *Electrochem. Commun.,* 2008, **10**, 1435.
[21] K. W. Nam, S. Kim, E. Yang, Y. Jung, E. Levi, D. Aurbach, J. W. Choi, *Chem. Mater.,* 2015. **27**. 3721
[22] S. Bach, J. Pereira-Ramos, N. Baffier, *J. power sources,* 1997, **68**, 586.

[23] B. Lanson, V. A. Drits, Q. Feng, A. Manceau, *Am. Minera.,* 2002, **87**, 1662.
[24] M. Tsuda, H. Arai, Y. Sakurai, *J. power sources,* 2002, **110**, 52.
[25] Y.-L. Chen, Y.-H. Hu, C.-A. Hsieh, J.-W. Yeh, S.-K. Chen, *J. Alloys Compd.,* 2009, **481**, 768.
[26] R. Gummow, A. De Kock, M. Thackeray, *Solid State Ionics,* 1994, **69**, 59.
[27] W. Li, J. Dahn, *J. Electrochem. Soc.,* 1995, **142**, 1742.
[28] Y. Liu, Y. Qiao, W. Zhang, H. Xu, Z. Li, Y. Shen, L. Yuan, X. Hu, X. Dai, Y. Huang, *Nano Energy,* 2014, **5**, 97.

Table of contents

Na-Birnessite with High Capacity and Long Cycle Life for Rechargeable Aqueous Sodium-ion Battery Cathode Electrodes

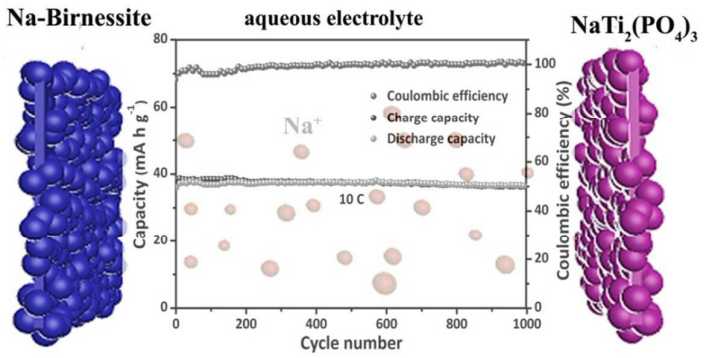

Na-Birnessite has been synthesized by a simple precipitation reaction at room temperature and exhibit high capacity of 39 mA h g^{-1} and long cycle life at 10 C in Na-Bir/$NaTi_2(PO_4)_3$ full cells.